A Neuro-Fuzzy Approach for Automatic Detection of Breast Cancer Based on Raman Spectroscopy

Francisco Javier Luna Rosas[1], **Julio Cesar Martínez Romo**[1], **Miguel Mora Gonzalez**[2], **Ricardo Mendoza Gonzalez**[1], **Valentín López Rivas**[1] **Gricelda Medina Veloz**[3]

[1] Computer Science Department, Inst. Tec. Aguascalientes, Aguascalientes, México.
[2] Centro Universitario de los Lagos, Universidad de Guadalajara, México
[3]Universidad Tecnológica del Norte de Aguascalientes, México

Abstract – *The harmful presence of cancerous cells in the feminine breast brings as a result, breast cancer, illness that has spread widely lately, not only in Mexico, but in other parts of the planet. In this paper we present a method of automatic Breast cancer classification, in which a Raman signal is classified as coming from a biopsy of healthy tissue (class ω_1) or biopsy of diseased tissue (class $\omega_{2)}$; to do so, we created patterns from Raman spectra accurately measuring each Raman peak to provide naturally reduced data to a classifier; we used Adaptative Neuro-Fuzzy Inference System (ANFIS) classifier and high rates of correct classification were obtained. This provides the specialists with important clinical tools for a rapid and efficient automatic detection of breast cancer. We consider that our approach can be applicable to other kinds of cancer, e.g., lung, prostate, stomach.*

Keywords: ANFIS, Breast Cancer, Raman Spectroscopy, Automatic Detection.

1 Introduction

Cancer is the 10th most common cause of death in the world [2], it is estimated that cancer will kill 83.2 million people in the world before the year 2015. Cancer is associated with the presence of more than one hundred specific related conditions that appear in a cell, the basic unit of life. Cancer takes place when cells begin to grow without any order and without control. When cancer appears, the cells keep on growing and multiplying although new cells are not needed. Generally, the change of a normal cell into a cancerous cell begins with mutations in the DNA in the nucleus of the cell, known as genome. There are many factors that allow the appearance of different types of cancer in women; one of the latter is breast cancer, and it is the most common type of cancer after lung cancer, (10.4 %, considering both sexes) and the fifth cause of death [3]. In adult women, breast cancer is the most common type of death, approximately 16 % [3]. There is a malignant tumor that begins in the bust cells (see Fig 1). This illness appears generally in women, but it is not exclusive, it can also appear in men. The main components of the female breast are lobules connected to the nipple by ducts, fat cells, blood vessels and lymphatic vessels. The function of the lymphatic ganglions is to fight bacteria, cancerous cells and other harmful substances to the organism. When the normal cycle of the cells fails and the new cells keep on growing or the old cells do not die, these cells form a deformed mass called tumor. These abnormal tissues called tumors qualify as benign tumors (are neither cancerous nor spread through the organism) and malignant (are cancerous and put life in danger).

The majority of the types of breast cancer begin in the conduits, in the lobes and in the bordering tissues. The cancerous cells are spread into the lymphatic ganglions next to the breast and to almost any part of the body such as bones, liver, lungs and to the brain itself.

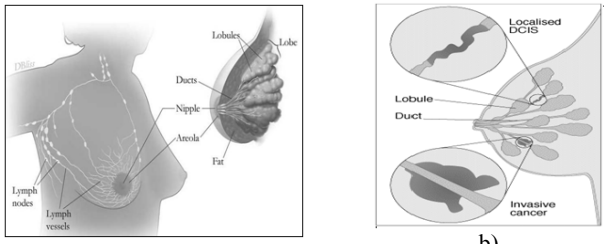

a) b)

Fig. 1. a) Feminine breast anatomy [1], b) Physical representation of Carcinoma ductal in situ (DCIS) [4]

1.1 Breast cancer types

There are several types of breast cancer [5], [3], [6]. **Ductal carcinoma in situ (DCIS)** is the most common type of non-invasive breast cancer where the cells of the ducts turn themselves into cancerous cells, (see fig. 1 b), and this is the first clinical diagnosis of breast cancer. **Lobular carcinoma in situ (LCIS):** [7], [8], begins in the milk-making glands but does not go through the wall of the lobules, (see Fig. 2a); although this is not a true cancer,

having LCIS increases a woman's risk of developing cancer later. When the carcinogenic cells acquire the ability of penetrating membranes, the cancer is named **Invasive ductal carcinoma (IDC),** (see Fig. 2b), and it can have access to the blood and the nodules; it means a potential spread to different organs of the body, for this reason, it is the most common type of invasive breast cancer. Another kind is **Invasive lobular carcinoma (ILC),** the tumor grows in the lobes of the breast and it can spread to other parts of the body too, generally, it does not appear in the screening analysis and it is only detected in the physical explorations.

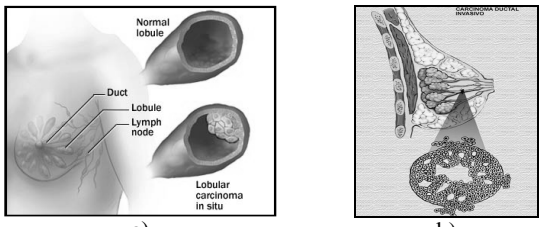

a) b)

Fig. 2. a) Physical representation of Lobular carcinoma in situ (LCIS) [9]. b) Physical representation of Invasive Ductual carcinoma zone (IDC) [10]

Other less common types of breast cancer that exist are: Inflammatory breast cancer (IBC), Fundamental Carcinoma, Illness of Paget of the nipple, Phyllodes Tumor and Tubular Carcinoma.

1.2 Physical examinations and screening

Early detection of breast cancer significantly reduces the risk of death. Tumors are found by physical examinations, by health professionals or by screening. Screening refers to checking for disease when there are no symptoms. Some screening tests and the current methods do not distinguish between a benign tumor and the malignant one, and for this reason they can be used to detect only suspicious injuries and not for diagnosis (to differentiate between a malignant or benign tumor at present specialized analyses through a biopsy are needed). Some tests are commonly used to screen for breast cancer, in this section some methods are mentoned. a) Breast self-exam (BSE) [12] and b) Clinical breast exam (CBE) [12] are exams made by the woman herself and by a health professional respectively, looking for lumps or anything else that seems unusual, c) Mammogram [11], [13] is an x-ray of the breast, it may find ductal carcinoma in situ (DCI), in symptomatic and asymptomatic women. d) Breast ultrasound [14] shows whether a lump is solid or fluid-filled. e) Magnetic Resonance Imaging (MRI) or (NMRI) [15], [16] a computer makes detailed pictures inside the breast area that show the difference between normal and diseased tissue.

1.3 Diagnosis

When the previous methods show abnormalities in the breast, some studies (tests) are made in tissues or blood samples to find whether the cells are cancerous. One of them is Breast biopsy or Tissue sampling (TS), [17], [18] where cells from breast tissue are examined under a microscope by a pathologist. With the purpose of limiting to the minimum the error of appreciation by the technician, alternative techniques of clinical diagnosis of breast cancer must be implemented. The use of optical diagnosis as the spectroscopy Raman [19] to provide additional information and to reinforce the diagnosis about the suspicious injury is an example. In recent years, several spectroscopic techniques such as Raman, Infrared and fluorescent have been used to examine tissues. Spectroscopy Raman (SR) uses beam laser that does not damage the cells of the tissue, but it provides information about its components [20], [21]; such is the case of cancerous tissues of breast [22], [23].

1.4 Raman Spectroscopy

The Raman Effect was described by Ch. V. Raman in 1982 [24]. The Raman spectroscopy analysis is a high-resolution technique that is based on the examination of the light dispersed by a material when affecting a monochrome beam of light; this provides chemical and structural information. Most of the dispersed light presents the same frequency that the incident light but a very small fraction displays a frequential change, result of the interaction of the light with the matter [24], [25]. The dispersed light that presents frequencies different from the incident radiation is that which provides information on the molecular composition of the sample (known as Raman dispersion).

1.5 Raman Spectroscopy and Breast Cancer

*Cancer Detection.*Various Raman spectroscopic studies on cancers have been reported, [26] and here we review one of the three most common cancers: breast cancer, the other two carcinomas (colorectal cancer and cervical cancer), are beyond the scope of this paper.

Breast Cancer. Breast cancer had the highest rate of occurrence in the United States among the female population in 2010 [26]. Numerous studies have investigated the application of Raman spectroscopy on the detection of normal, precancerous and cancerous breast tissues. For instance, Haka [27] and colleagues have demonstrated the ability of Raman spectroscopy to distinguish between normal, benign, and malignant lesions of breast ex vivo, with a sensitivity of 94% and a specificity of 96%. Tissues in four pathological conditions were examined and classified, including normal, fibrocystic change, fibroadenoma, and infiltrating carcinoma. Raman

spectra of breast tissues were fitted to those of individual breast tissue components including fat, collagen, cell nucleus, epithelial cell cytoplasm, calcium oxalate, calcium hydroxyapatite, cholesterol-like lipid deposits, and β-carotene. Instead of examining breast tissues directly, Pichardo-Molina's group [28] studied serum samples from breast cancer patients and demonstrated the use of Raman spectroscopy for minimally invasive diagnostics. Seven Raman band ratios were used for classification, and spectral differences were observed between serum samples of breast cancer patients and normal healthy subjects. Using principal component analysis (PCA) and linear discriminant analysis (LDA), the sensitivity and specificity were reported to be 97% and 78%, respectively. However, the underlying molecular mechanism of these differences was not reported. Raman spectroscopic imaging technique has gained popularity recently in cancer research. Raman spectroscopic imaging is capable of visualizing the samples without extrinsic labeling, thus minimizing sample perturbation. In addition, the much-needed chemical and structural information about the sample are provided by Raman spectral analysis. Mariani and coworkers have applied Raman imaging to the detection of nuclear membrane lipid fluctuations in senescent epithelial breast cancer cells [28]. In this study, Raman images were composed based on the Raman peak intensity of CH-stretching. Another example is the proposed Abramczyk [30], in their study presents the most reliable statistical analysis based on Raman spectroscopy, data of normal breast tissue, benign and cancerous of 146 patients were found. In his article presents the first Raman optical biopsy images (RI) from normal and cancerous breast tissues from the same patient. The results presented demonstrate the ability of Raman spectroscopy to characterize exactly types of tissue (non-cancerous) or cancerous. The results provide evidence that the composition of lipids and carotenes differ significantly from non-cancerous and cancerous breast tissue that should be a key factor in the mechanisms that detect cancer.

Analysis methods. Raman spectra obtained from biological samples often contain significant amounts of fluorescence background. As Raman spectral differences between normal and diseased tissues are generally subtle, effective data-processing algorithms are often required for data analysis and interpretation.

Fluorescence background removal. As mentioned above, Raman spectra collected from tissues are composed mainly of Raman scattering and intrinsic tissue fluorescence. To eliminate the fluorescence background, a polynomial function that fits to the fluorescence profile is usually subtracted from the Raman spectra [31]. Although there is no consensus on the optimal order of the polynomial function, fourth- and fifth-order polynomials are most commonly employed [31].

Multivariate data analysis. Raman spectra contain various overlapping Raman bands. As a result, it is difficult to visually inspect and interpret the spectral data. Multivariate spectral analysis methods are often used to process the Raman spectra and facilitate data interpretation. Spectral analysis methods are generally categorized as either supervised or unsupervised. For unsupervised analyses, such as cluster analysis and PCA [28], no a priori knowledge of class characteristics is required but is to be determined from the analysis itself. In contrast, in a supervised analysis the number of classes and representative samples of each class are known a priori, as is the case in LDA [28], regression analysis, and artificial neural networks (ANNs).

2 Experimental methods

2.1 Subjects and protocol

Raw Raman spectra (Raman scattering plus background fluorescence) were provided to us by the Research Center in Optics (CIO, Centro de Investigaciones en Óptica, A.C.), and were taken from samples of cancerous and healthy breast tissue provided by the Cancer Institute of Jalisco, México; the samples were obtained by excisional biopsy of patients diagnosed with infiltrating ductal cancer and preserved in formalin; in order to obtain the Raman spectra, histological cuts were made on the samples. The Raman spectra were obtained using a Raman Renishaw system model 1000-B; this system uses a laser diode of λ = 830 nm and a grating of 600 lines mm-1. The laser was focused on the samples with a Leica microscope model DMLM (objective of 50x), at approximately 35mW of power. Each spectrum was collected in the region from 680 to 1780 cm-1, with an exposition time of 10s. Finally, the wavenumber resolution was of 2 cm-1 and the Raman system was calibrated with a silicon semiconductor at the Raman peak in 520 cm-1. With this experimental setup 100 Raman spectra were recorded from healthy and diseased tissue zones of the biopsies. For fluorescence removal, in this work, we adopted the Vancouver Raman Algorithm (VRA) [37], because it avoids the possible oscillations at the extreme points of the spectrum that other algorithms insert to the corrected Raman spectrum.

3 Results and Discussion

3.1 Highlighting Differences Raman Spectrum of Healthy Tissue Vs. Raman Spectrum of Damaged Tissue

In this section we present the results of Raman studies on normal breast tissue (noncancerous) and damaged

(cancerous). Previous publications [30], [28], [33] have demonstrated that the Raman spectrum of normal breast tissue are dominated by lipids and carotenes. Healthy tissue spectrum show peaks in the bands 1004, 1080, 1158, 1259, 1266, 1304, 1444, 1518, 1660, 1750 and damaged tissue (cancerous tumors, invasive ductal carcinoma) gets less peak intensity. Fig. 3 compares a Raman spectrum of healthy and damaged breast tissue from the same patient. The most notorious differences can be observed in the regions of the bands 1158 and 1518 cm-1 assigned to carotenoids [30] and the regions of the bands 1444, 1660, 1750 cm-1that have been assigned to the lipids. A detailed inspection in Fig. 3 demonstrates that the Raman bands of the carotenoids are strong in healthy tissue while in damaged tissues they are not seen. Raman intensities of the peaks of lipids are significantly smaller in damaged tissue than in healthy tissue (bands 1444, 1750, 1259.1080) [30].

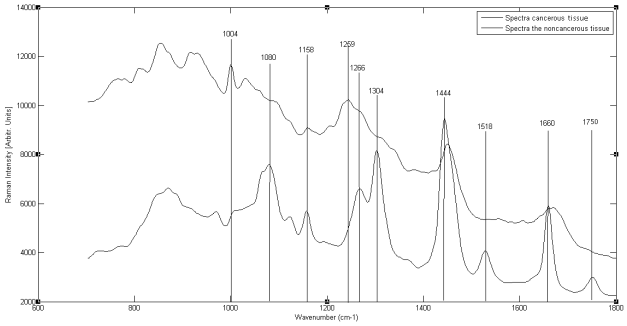

Fig. 3. Raman Spectrum of Normal and Damaged Breast Tissue (Invasive Ductal Carcinoma) of the Same Patient.

3.2 Analysis of Components Multivariate

Recently, multivariate methods have been applied to Raman spectroscopy to classify breast cancer tissue, noncancerous and cancerous. In Particular way the principal component analysis (PCA) has been used to differentiate healthy and damaged tissue [34].

Table 1. Feature Vectors for 86 Raman Spectrum Healthy and Damaged Breast Tissue.

Raman Scatter Region									
Region(Wavenumber in cm^{-1})									
1750	1660	1518	1444	1304	1266	1259	1158	1080	1004
0	1027.9	0	2011.2	0	0	469	0	0	403
0	782.1	0	1704	0	0	447	0	0	251
0	1597	0	3020	0	0	1154	0	0	1193
…	…	…	…	…	…	…	…	…	…
…	…	…	…	…	…	…	…	…	…
0	2408	0	4551	0	0	2171	0	0	1398
0	3070	0	5205	0	0	2004	0	0	1535

PCA is a multivariate technique that acts in an unsupervised manner, and is used to analyze the inherent structure of the data. PCA reduces the dimensionality of the data set to obtain an alternative set of coordenates: principal components (PCs). PCs are linear combinations of original variables which are orthogonal and are designed so that each one has the maximum variability in the data set [28].
As each of the spectrum contains a large amount of information we needed PCA help to extract important features or components. In PCA method each Raman spectrum is represented as a vector of intensity values of each wavelength. To make the multivariate component analysis (PCA), we obtained the Raman peak intensities of both healthy tissue and damaged tissue of the same patient´s biopsy. 86 vectors were formed with a features length ($\lambda = 10$), each feature is based on peaks intensity of the of their respective wave number (cm-1) as shown in Table 1. Once the feature vectors extracted from the 86 spectra based on Raman peak Intensities, we proceeded to a dimensions reduction, on which feature vectors that describe to Raman spectrum of healthy breast tissue as well as tissue damaged breast (Table 2).

Table 2. Principal Component Analysis in Three Dimensions.

Spectrum	pc1	pc2	pc3
1	523	-425	131
2	1223	-602	290
3	2137	-877	295
…	…	…	…
…	…	…	…
85	-1028	-503	3
86	-1053	-448	17

Fig 4 shows the new feature vectors distribution of Raman spectrum in the 86 tri-dimensional space in the first 3 principal components obtained from different parts of a breast cancer biopsy.

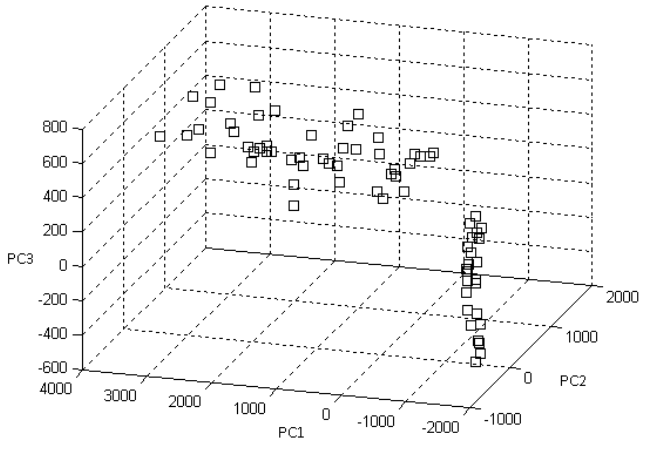

Fig. 4. PCA in Three Dimensions Retrieved from the Intensities of the Peaks Detected in Raman Spectrum 86.

3.3 Algorithm K-Means Clustering

Generally, PCA analysis by itself does not provide the meaning answer that each PCA component have, because the PCA does not group (Clustering) only reduces dimensions K-means is a clustering algorithm, which is an easy way to divide a given database in k groups (determined a priori).The main idea is to define k centroids (one for each group of the database and place them in the type of its nearest centroid. Next step is to recalculate the centroid of each group and redistribute all items according to the nearest centroid. The process is repeated until there are no changes in the groups from one step to the next. Detailed inspection of the algorithm can be observed in [35]. We apply the K-means algorithm to find the distribution of two kinds in our case these two kinds will be healthy breast tissue and damage breast tissue. For convenience each kind will be expressed as ω_1 and ω_2 respectively.

ω_1 = Healthy breast tissue.
ω_2 = Damaged breast tissue.

The K-means algorithm after 10 iterations grouped 44 feature vectors type ω_1 and 42 in ω_2 (Table 3). In the first column of Table 3 it´s shown the type to which belongs each feature vector of the Raman spectrum of healthy and damaged tissue.

Table 3. Structure for Feature Vectors

Class	Vector	Spectrum	pc1	pc2	pc3
ω_1	1	82	-1025	489	85
ω_1	2	83	-1074	815	30
ω_1	3	84	-1081	827	46
…	…	…	…	…	
…	…	…	…	…	…
ω_1	43	85	-1028	503	3
ω_1	44	86	-1053	448	17
ω_2	45	1	523	-425	131
ω_2	46	2	1223	-602	290
ω_2	47	3	2137	-877	295
…	…	…	…	…	…
…	…	…	…	…	…
ω_2	85	85	-1028	-503	3
ω_2	86	86	-1053	-448	17

The distribution of both types is shown in Fig. 5, as we can see in Fig. 5, the examples are from one of two distinctive groups, the left and right circles are separated according to healthy and damaged tissue. The left side circle exclusively represents normal breast tissue. The right circle represents damaged tissue.

Once the data is clustered the 86 Raman spectra are verified, Raman spectrum of normal breast tissue can be observed in Fig. 6 (a) and Raman spectrum of damage breast tissue can be seen in Fig. 6 (b).

Fig. 6 (a) and (b) clearly show many marked differences in the Raman spectrum of healthy and damaged tissue. The peaks of the Raman bands 1004, 1080, 1158, 1259, 1266, 1304, 1444, 1518, 1660, 1750 that have been assigned to lipids and carotenes are significantly different in healthy and damaged breast tissue.

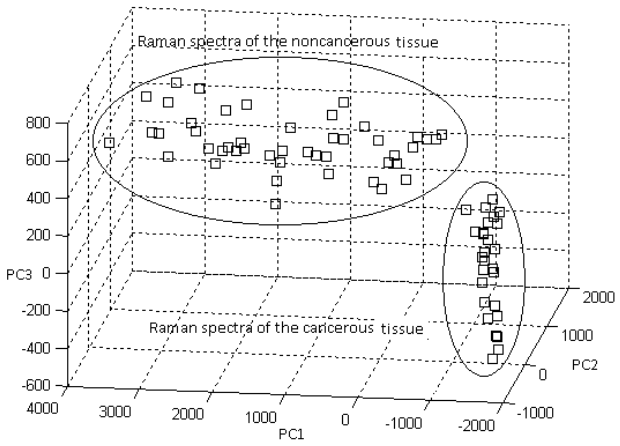

Fig. 5. Grouping of 86 Raman Spectrum with Healthy Breast Tissue (Left Side) and Breast Tissue with Invasive Ductal Carcinoma (Right Side).

As there are many marked differences in the Raman spectra of healthy and damaged breast tissue we considerate a Neuro-diffuse classifier (ANFIS).

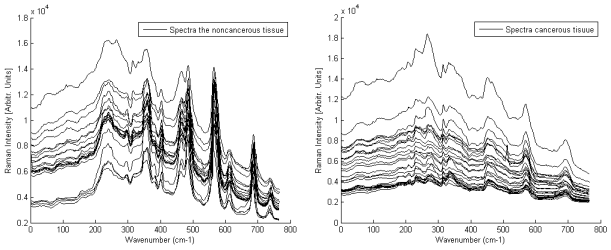

a) b)

Fig. 6. Raman Spectra of Healthy and Damage Breast Tissue Result of the Clustering Algorithm K-means Type.

As there are many marked differences in the Raman spectra of healthy and damaged breast tissue we considerate a Neuro-diffuse classifier (ANFIS).

3.4 ANFIS Architecture

Adaptative Neuro Fuzzy Inference System (ANFIS) is an architecture that is functionally equivalent to diffuse inferential systems (fuzzy), that is to say, is equivalent to the type of diffuse rules base of Takagi and Sugeno [36]. In the next section you will see results of ANFIS obtained from the evaluation of the 45 feature vectors of healthy tissue Raman spectra in Class ω_1 and 45 vectors of

damaged tissue spectra associated with the class ω_2, using the technique of cross-validations. To evaluate the correct classification percentage it was performed the following confusion matrix:

Table 4. Confusion Matrix.

Class	ω_1	ω_2
ω_1	$VN_{(1,1)}$	$FP_{(1,2)}$
ω_2	$FN_{(2,1)}$	$VP_{(2,2)}$

Where:

TN (True Negative). The disease is not present and diagnosed as healthy.
FP (False Positive). The disease is not present and it´s diagnosed ill.
FN (False Negative). The disease is present but not detected.
TP (True Positive). The disease is present and detected.

Considering the confusion matrix previously described we can assess the *sensitivity* of our classifier to detect positive case of ill patients (percentage of patients correctly identified) and *specificity* that indicates the ability of our classifier to give as negative cases really healthy cases (percentage of correctly identified healthy patients).

$$Sensibilidad = \frac{VP}{VP + FN} * 100 \quad (1)$$

$$Especificidad = \frac{VN}{VN + FP} * 100 \quad (2)$$

The ANFIS classifier was evaluated with the membership functions Triangular, Trapezoidal, Gaussian and Bell. Having each one 10, 100 and 250 training epochs while fixing a threshold for classification. Table 5 shows the sensitivity and specificity of ANFIS classifier using the membership functions mentioned above.

Table 5. Sensitivity, Specificity and Predictive Accuracy Through ANFIS.

Membership Fuctions	**Errors (case 18 bands + ANFIS)**		**Sensitivity**	**Specificity**
	Healthy as cáncer(FP)	Cancer as healthy(FN)		
Triangular Membership	0/45	1/45	100%	97.77%
Trapezoid Membership	1/45	1/45	97.77%	97.77%
Gaussian Membership	1/45	2/45	97.77%	95.55%
Bell-shape Membership.	2/45	1/45	95.55%	97.77%

Fig. 8 shows the ANFIS classifier with a triangular membership function and 100 training epochs, in the figure we can observe that the classifier achieved a sensitivity of 100% and a specificity of 97.77%, with a classification error of 0% False Negatives (FN) and 2.23% for False Positives (FP).

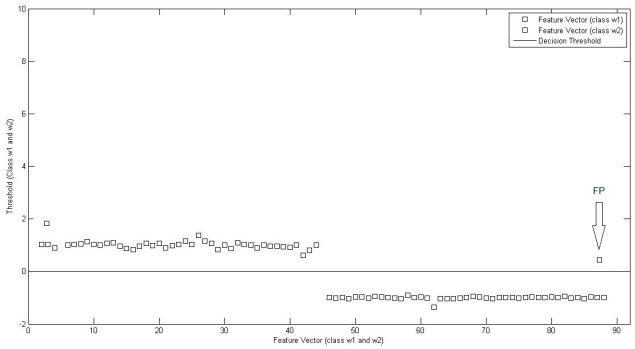

Fig. 8. Decision Threshold ANFIS with Triangular Membership Function 100 Epochs.

4. Conclusions

In this article we present a method for the automated detection of breast cancer in which a Raman signal is classified as healthy tissue biopsy (class ω_1) and damage tissue (type ω_2). An important aspect is the characteristic generating, using PCA, in the PCA method each Raman spectrum was represented as a vector of values of intensity for each wavelength, that represent Raman peaks both healthy tissue and damaged tissue. PCA analysis by itself does not provide the answer meaning that each component PCA have, as the PCA does not group (Clustering) only reduces the dimensions. We apply the K-means algorithm to find the distribution of two types, in our case these two types were damaged tissue and healthy tissue. For convenience each type was expressed as ω_1 and ω_2 respectively, after detecting types we tried a Neuro-diffuse classifier (ANFIS) and high correct classification rates were obtained.

5. References

[1] This National Cancer Institute (NCI) booklet (NIH Publication No. 05-1556). National Cancer Institute. (www.cancer.gov).
[2] An update of the global burden of disease in 2004. Geneva, World Health Organization (forthcoming).
[3] World Health Statistics, 2008. World Health Organization 2008. ISBN 978 92 4 156359 8.
[4] Ernster VL, Ballard-Barbash R, Barlow WE, et al (Oct 2002). "Detection of ductal carcinoma in situ in

women undergoing screening mammography". J Natl Cancer Inst 94 (20): 1546–54.
[5] Breast Cancer document. Technical Report. American Cancer Society. (www.cancer.org).
[6] Tumours of the breast and female genital organs, WHO. Classification of tumours, 2003.
[7] Foote FW, Stewart FW. Lobular carcinoma in situ: a rare form of mammary cancer. Am J Pathol1941; 17:491-496.
[8] Hutter RVP, Foote FW. Lobular carcinoma in situ. Long term follow-up. Cancer. 1969; 24, 1081.
[9] Causes of Lobular Carcinoma in situ. Mayo Foundation for Medical Education and Research (MFMER). Technical Report. (MayoClinic.com)
[10] Tests for Diagnosing IDC. www.breastcancer.org
[11] Breast cancer screening. Lyon, International Agency for Research on Cancer, 2002 (Handbooks on Cancer Prevention, Vol. 10)
[12] International Agency for Research on Cancer IARC. Technical Report. (screening.iarc.fr/)
[13] National Cancer Institute. Breast Cancer: Screening and Testing. Bethesda, MD: National Cancer Institute. Accessed: 25 September 2008. (www.cancer.gov)
[14] Wilson ARM. Ultrasound guidance boosts biopsy outcome. Diagnostic Imaging Europe: 40-45 & 50, December 1999.
[15] Lauterbur, P.C. (1973). "Image Formation by Induced Local Interactions: Examples of Employing Nuclear Magnetic Resonance". Nature 242: 190-191.
[16] Gould, RT-(R)(MR)(ARRT), Todd A. "How MRI Works." 01 April 2000. HowStuffWorks.com. (www.health.howstuffworks.com)
[17] Abeloff MD, Armitage JO, Niederhuber JE, Kastan MB, McKena WG. Clinical Oncology. 3rd ed. Orlando, Fl: Churchill Livingstone; 2004
[18] Whitman GJ. Ultrasound-guided breast biopsies. Ultrasound Clin. Dec 2006; 1(4); 603-615.
[19] K. E. Shafer-Peltier, A. S. Haka, M. Fitzmaurice, J. Crowe, J. Myles, R. R. Dasari, M. S. Feld, J. Raman Spectrosc. 33 (2002) 552.
[20] Parker FS (1983) Applications of infrared Raman, and resonance Raman spectroscopy in biochemistry. Plenum, New York.
[21] Das K, Stone N, Kendall C, Fowler C, Christie-Brown J. (2006) Raman spectroscopy of parathyroid tissue pathology. Lasers Med Sci 21(4):192–197
[22] Alfano RR, Liu CH et al (1991) Human breast tissue studied by IR Fourier transform Raman spectroscopy. Lasers in Life Sci 4:23–28
[23] Pichardo-Molina, et all. Raman spectroscopy and multivariate analysis of serum samples from breast cancer patients. (2006) Lasers Med Sci. DOI 10.1007/s10103-006-0432-8., Springer-Verlag.
[24] Raman, C. V., Nature, 108, 367, 1921
[25] C. V. Raman, K.S. Krishnan, A new type of Secondary Radiation, Nature, 121, 619, 1928.
[26] Qiang Tu, MS, Chang Chang. Diagnostic applications of Raman spectroscopy. Nanomedicine: Nanotechnology, Biology, and Medicine 8 (2012) 545–558.
[27] Haka AS, Shafer-Peltier KE, Fitzmaurice M, Crowe J, Dasari RR, Feld MS. Diagnosing breast cancer by using Raman spectroscopy. Proc Natl Acad Sci U S A 2005;102:12371-6.
[28] Pichardo-Molina JL, Frausto-Reyes C, Barbosa-Garcia O, Huerta-Franco R, Gonzalez-Trujillo JL, Ramirez-Alvarado CA, et al. Raman spectroscopy and multivariate analysis of serum samples from breast cancer patients. Lasers Med Sci 2007;22:229-36.
[29] Mariani MM, Maccoux LJ, Matthaus C, Diem M, Hengstler JG, Deckert V. Micro-Raman detection of nuclear membrane lipid fluctuations insenescent epithelial breast cancer cells. Anal Chem 2010;82:4259-63.
[30] Abramczyk Halina, Beata Brozek-Pluska, Jakub Surmacki, Joanna Jablonska-Gajewicz, Radzislaw Kordek. Raman 'optical biopsy' of human breast cancer. Progress in Biophysics and Molecular Biology. 108(2012) 74-81.
[31] Tu Q, Eisen J, Chang C. Surface-enhanced Raman spectroscopy study of indolic molecules adsorbed on gold colloids. J Biomed Opt 2010;020512:15.
[32] Robichaux-Viehoever A, Kanter E, Shappell H, Billheimer D, Jones III H, Mahadevan-Jansen A. Characterization of Raman spectra measured in vivo for the detection of cervical dysplasia. Appl Spectrosc 2007;61:986-93.
[33] B. Brożek-Płuska, I. Placek, K. Kurczewski, Z. Morawiec, M. Tazbir, H. Abramczyk. Breast cancer diagnostics by Raman spectroscopy, Journal of Molecular Liquids 141 (2008) 145–148
[34] H. Abramczyk, J. Surmacki, B. Bro_zek-Płuska Z. Morawiec M. Tazbir. The hallmarks of breast cancer by Raman spectroscopy, Journal of Molecular Structure 924–926 (2009) 175–182.
[35] K. Koutroumbas y S. Theodoridis, Pattern Recognition, 1st ed. California, E. U. A.: Academic Press, 1999.
[36] Roger, J.S., 1997. Neuro-fuzzy and Soft Computing. Prentice Hall. Nj, USA. ISBN 0-13-261066-3.
[37] J. Zhao, H. Lui, D. I. McLean, y H. Zeng, "Automated autofluorescence background subtraction algorithm for biomedical Raman spectroscopy", *Applied Spectroscopy*, vol. 61, no. 11, p. 1225–1232, 2007.